



The Bolund experiment - design of measurement campaign using CFD

Bechmann, Andreas; Johansen, Jeppe; Sørensen, Niels N.

Publication date:
2007

Document Version
Publisher's PDF, also known as Version of record

[Link back to DTU Orbit](#)

Citation (APA):
Bechmann, A., Johansen, J., & Sørensen, N. N. (2007). *The Bolund experiment - design of measurement campaign using CFD*. Risø National Laboratory. Denmark. Forskningscenter Risoe. Risoe-R No. 1623(EN)

General rights

Copyright and moral rights for the publications made accessible in the public portal are retained by the authors and/or other copyright owners and it is a condition of accessing publications that users recognise and abide by the legal requirements associated with these rights.

- Users may download and print one copy of any publication from the public portal for the purpose of private study or research.
- You may not further distribute the material or use it for any profit-making activity or commercial gain
- You may freely distribute the URL identifying the publication in the public portal

If you believe that this document breaches copyright please contact us providing details, and we will remove access to the work immediately and investigate your claim.

The Bolund Experiment - Design of Measurement Campaign using CFD

Andreas Bechmann, Jeppe Johansen and Niels N. Sørensen

Risø-R-1623(EN)

Author: Andreas Bechmann¹, Jeppe Johansen¹, Niels N. Sørensen^{1,2}
Title: The Bolund Experiment - Design of Measurement Campaign using CFD
Department (1): Wind Energy Department
Department (2): Department of Civil Engineering, Aalborg University

Abstract (max. 2000 char.):

The Bolund experiment is a study of the flow over Bolund, a small hill located near Risø DTU. In the present work, the flow over the Bolund hill has been computed using the EllipSys3D Navier-Stokes solver. The aim of this work is to identify the flow conditions at the hill in order to prepare the upcoming measurement campaign. The simulation results are used for estimating rational positions of measuring masts and instrumentation. A total of ten measuring masts are proposed consisting of two 16 m masts, six 9 m masts and two 5 m masts. The masts are instrumented with 12 cup anemometers for mean wind measurements and 21 sonics for 3-component turbulence measurements.

Risø-R-1623(EN)
December 2007

ISSN 0106-2840
ISBN 978-87-550-3638-3

Contract no.:
ENS-33033-0062

Group's own reg. no.:
1110058-01

Sponsorship:
Energistyrelsen
Danish Energy Agency

Cover :

Pages: 19
Tables: 1
References: 9

Information Service Department
Risø National Laboratory
Technical University of Denmark
P.O.Box 49
DK-4000 Roskilde
Denmark
Telephone +45 46774004
bibl@risoe.dk
Fax +45 46774013
www.risoe.dk

Contents

Preface 4

1 Bolund hill 5

- 1.1 Objective 5
- 1.2 Site description 5
- 1.3 Simulation methodology 6

2 Computational solver 8

3 Computational grid 9

- 3.1 Gridded file 9
- 3.2 Surface grid 11
- 3.3 Volume grid 12

4 Boundary conditions 13

- 4.1 Inlet and top 13
- 4.2 Outlet 13
- 4.3 Wall 13

5 Results 14

- 5.1 Flow visualisation 14
- 5.2 Location of measuring masts 15
- 5.3 Instrumentation 16

6 Discussion 18

Acknowledgement 18

References 19

Preface

The present report describes the simulation methodology and results of initial CFD computations of the wind conditions over the Bolund hill. The simulations have been conducted before an upcoming measuring campaign in order to estimate the best possible positions for measuring equipment.

The work is conducted under the EFP project:

EFP07 - Metoder til kortlægning af vindforhold i komplekst terræn. (ENS-33033-0062)



Figure 1. Left: The Bolund hill is located north of Risø DTU. Right: Aerial close-up of Bolund. (from Google Earth)

1 Bolund hill

1.1 Objective

The main objective of the Bolund experiment is to increase knowledge of atmospheric boundary-layer flows in complex terrain with the main focus on applications related to siting of wind turbines. Additionally, reliable methods for determining local wind conditions based on remote sensing techniques in combination with advanced flow computations will be developed.

The Bolund hill is located just north of Risø DTU National Laboratory for Sustainable Energy, Roskilde, Denmark. The site has been selected for a detailed measurement campaign, which will provide detailed knowledge of the local wind conditions as well as resulting in a unique dataset for validating advanced flow models.

Thorough measurements of mean velocity and turbulence profiles at different positions using sonic and cup anemometers together with Lidar are expected to give detailed insight to the complex flow. The present report describes preliminary CFD simulations of the wind over Bolund. Based on simulation results positions of the measurement masts used in the field experiment are found.

1.2 Site description

Bolund is a 12m high, 130m long and a 75m wide costal hill located just north of Risø DTU (see Figure 1). The Bolund hill is too small to represent a wind turbine site. However, the geometrical shape of the hill consists of properties that characterize a complex terrain. Properties like the well-exposed steep upstream escarpment (see Figure 2). The Bolund experiment can therefore be described as a scaled down version of a real wind turbine site.

There are several reasons for selecting Bolund for the field experiment:

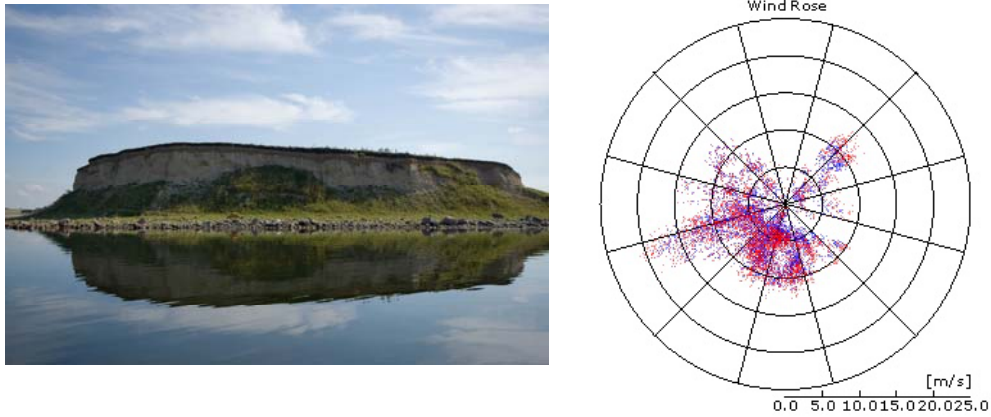


Figure 2. Left: The steep escarpment of Bolund seen from the west. Right: Wind rose

1. The hill is surrounded by water with a long uniform upstream fetch (sea) of approximately 7 km with wind from the west (270-direction) and 4 km when the wind comes from south-west (240-direction). Having a long upstream fetch ensures that the incoming wind is in a state of equilibrium and is horizontally homogeneous. This ensures that the whole of the Bolund hill experiences the same inflow.
2. The relatively low height of Bolund (12 m) ensures that most of the daytime measurements are performed in the surface-layer, which is the bottom part of the atmospheric boundary-layer layer. Turbulence is mainly mechanically generated by the wind shear in the surface-layer, and conditions can therefore often be considered near-neutral. Additionally, Coriolis effects can be ignored in the surface-layer.
3. The ground of Bolund is uniformly covered by grass and the wind is not influenced from any individual roughness elements.

From a numerical modeling point of view, this isolation and relative simple attributes are appropriate features. Finally, the proximity to Risø makes the hill easily accessible from Risø, which is a clear advantage when performing measurements.

A wind rose measured during one month, September 2007, at the Risø measurement mast is shown on Figure 2. The wind rose shows that the predominant wind direction is from west south-west. The field experiment needs to be set up with this wind direction in mind.

1.3 Simulation methodology

CFD simulations of the wind over Bolund hill for various wind directions have been performed. Initially, four wind directions were simulated: wind from north, south east and west (360, 180, 90 and 270 degrees). Since the predominant wind direction is from west south-west, an extra direction (240 degrees) was simulated.

Here, only results from the 270 and 240 wind-directions are presented, since the mast positions mainly are determined based on those directions.

This report first describes the flow solver EllipSys3D that has been used in all computations. Secondly, the generation of the computational grid is described. This is an important part of any CFD simulation and is therefore thoroughly described. Thirdly, the used boundary conditions are explained and finally simulation results with proposed mast positions are given.

2 Computational solver

The in-house flow solver EllipSys3D is used in all computations presented in the following. The code is developed in co-operation between the Department of Mechanical Engineering at DTU and The Department of Wind Energy at Risø National Laboratory, see [1] [2] and [3]. The EllipSys3D code is a multiblock finite volume discretization of the incompressible Reynolds Averaged Navier-Stokes (RANS) equations in general curvilinear coordinates. The code uses a collocated variable arrangement, and Rhie/Chow interpolation is used to avoid odd/even pressure decoupling. As the code solves the incompressible flow equations, no equation of state exists for the pressure, and in the present work the SIMPLE algorithm of [6] is used to enforce the pressure/velocity coupling. The EllipSys3D code is parallelized with MPI for executions on distributed memory machines, using a non-overlapping domain decomposition technique.

Both steady state and unsteady computations can be performed. For the unsteady computations the solution is advanced in time using a 2nd order iterative time-stepping (or dual time-stepping) method. In each global time-step the equations are solved in an iterative manner, using under relaxation. First, the momentum equations are used as a predictor to advance the solution in time. At this point in the computation the flow field will not fulfill the continuity equation. The rewritten continuity equation (the so called pressure correction equation) is used as a corrector making the predicted flow field satisfy the continuity constraint. This two step procedure corresponds to a single sub-iteration, and the process is repeated until a convergent solution is obtained for the time step. When a convergent solution is obtained, the variables are updated, and we continue with the next time step. For steady state computations, the global time-step is set to infinity and dual time stepping is not used, this corresponds to the use of local time stepping. In order to accelerate the overall algorithm, a multi-level grid sequence is used in the steady state computations.

The convective terms are discretized using a third order QUICK upwind scheme, implemented using the deferred correction approach first suggested by Khosla and Rubin [7]. Central differences are used for the viscous terms, in each sub-iteration only the normal terms are treated fully implicit, while the terms from non-orthogonality and the variable viscosity terms are treated explicitly. Thus, when the sub-iteration process is finished all terms are evaluated at the new time level. The three momentum equations are solved decoupled using a red/black Gauss-Seidel point solver. The solution of the Poisson system arising from the pressure correction equation is accelerated using a multigrid method.

In the present work the turbulence in the boundary layer is modeled by the RANS $k-\epsilon$ eddy viscosity model of [8], with constants calibrated for atmospheric conditions, as described in [3]. Additional simulations using an unsteady hybrid RANS/LES method [9] have also been conducted. However, since these results are very similar to the ones achieved with the RANS method, only steady state RANS computations are presented in this work.

3 Computational grid

The computational grid is a very important part of any CFD simulation and in the present application the following three step procedure is used. First a gridded Cartesian file of terrain heights is constructed based on measured terrain heights. Secondly, a surface mesh of the whole computational domain is generated and thirdly the final volume mesh is constructed.

3.1 Gridded file

Terrain measurements have been performed by COWI with accuracy of 15cm vertically and 10cm horizontally and with a horizontal resolution of about 2mx2m. The measurements are unstructured and need to be gridded.

```
X (east)  Y(north)  Z (height)
694874.01  6177311.19  0.58
694873.80  6177313.56  0.66
694874.28  6177314.77  0.55
694874.29  6177316.30  0.68
694873.81  6177315.11  0.51
694872.85  6177312.68  0.53
694872.37  6177311.48  0.53
694870.57  6177310.51  0.80
694871.03  6177311.69  0.62
694871.50  6177312.89  0.59
694871.98  6177314.09  0.53
694872.45  6177315.29  0.55
...
```

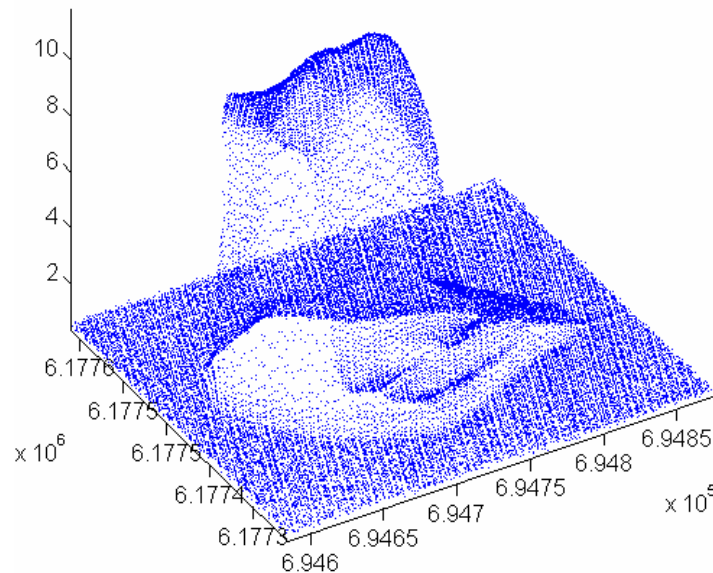


Figure 3. Extract of the COWI measurements (DTM_RAW_utm32_euref89_DVR90.xyz).

In order to grid the measured data, the x- and y-coordinates are translated so that new coordinate centre is placed at (694684.12; 6177444.9). This is necessary in

order to maintain numerical precision. The actual gridding was done using the MatLab function “griddata” using 390x390 grid points covering an area of 290m times 250m. “Griddata” used a triangle-based linear interpolation. The resolution is somewhat higher than the measured data in order maintain precision. Secondly the region that represents the water surface was smoothed out to a height of 0.75m, thereby achieving a constant surface height at the grid edges. This is convenient when generating the actual surface grid – for instance if cyclic boundary conditions need to be used. Thirdly, the gridded data was smoothed once by applying a 1:2:1 smoothing operator to the surface-height values. This was done in order to remove small unphysical fluctuations that might be present from measurement inaccuracies or from the interpolation used.

X (east)	Y(north)	Z (height)
-1.0000000e+002	-1.3000000e+002	7.5000000e-001
-9.9253393e+001	-1.3000000e+002	7.5000000e-001
-9.8506787e+001	-1.3000000e+002	7.5000000e-001
-9.7760180e+001	-1.3000000e+002	7.5000000e-001
-9.7013573e+001	-1.3000000e+002	7.5000000e-001
-9.6266967e+001	-1.3000000e+002	7.5000000e-001
-9.5520360e+001	-1.3000000e+002	7.5000000e-001
-9.4773753e+001	-1.3000000e+002	7.5000000e-001
-9.4027147e+001	-1.3000000e+002	7.5000000e-001
-9.3280540e+001	-1.3000000e+002	7.5000000e-001
-9.2533933e+001	-1.3000000e+002	7.5000000e-001
-9.1787326e+001	-1.3000000e+002	7.5000000e-001
...		

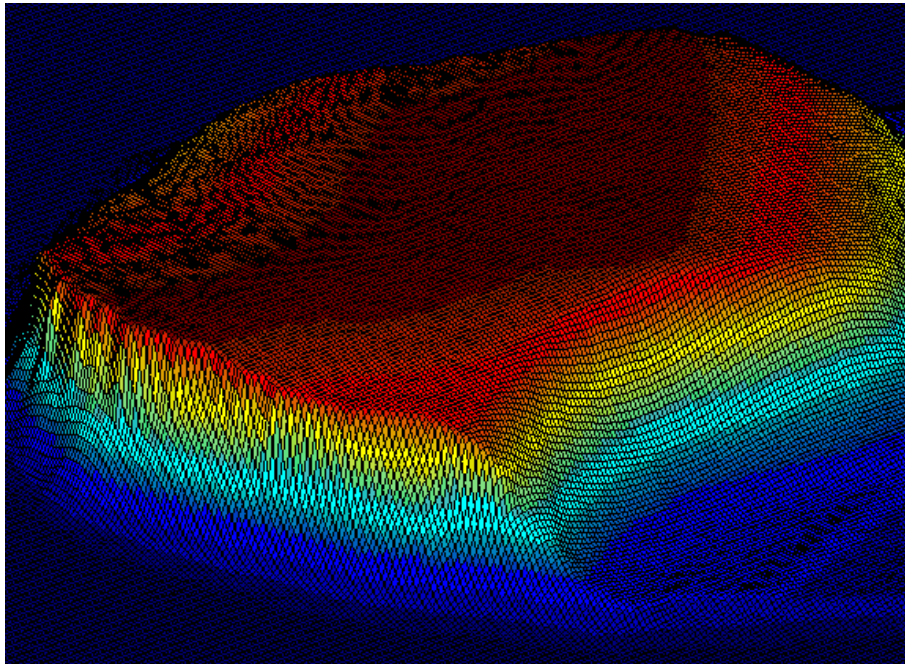


Figure 4. Extract and plot of the gridded data.

3.2 Surface grid

Based on the gridded terrain file a surface grid is constructed using the program “GridGen”. Since the wind is mainly from the east (270), the surface grid is constructed specifically for this wind direction – ensuring a long stretch both up- and downstream of the hill (about four hill lengths). The grid is aligned with the main flow direction – this minimizes numerical diffusion. The grid’s outer dimension is $1.1 \text{ km} \times 0.7 \text{ km}$ using 18 blocks of 48^2 cells with typical cell dimensions on the hill of $2.5 \text{ m} \times 0.8 \text{ m}$. The surface grid is refined towards the hill with a topology that ensures that grid lines are aligned with the hill slope. Grid cells with a high degree of orthogonality are thereby achieved (see figure below).

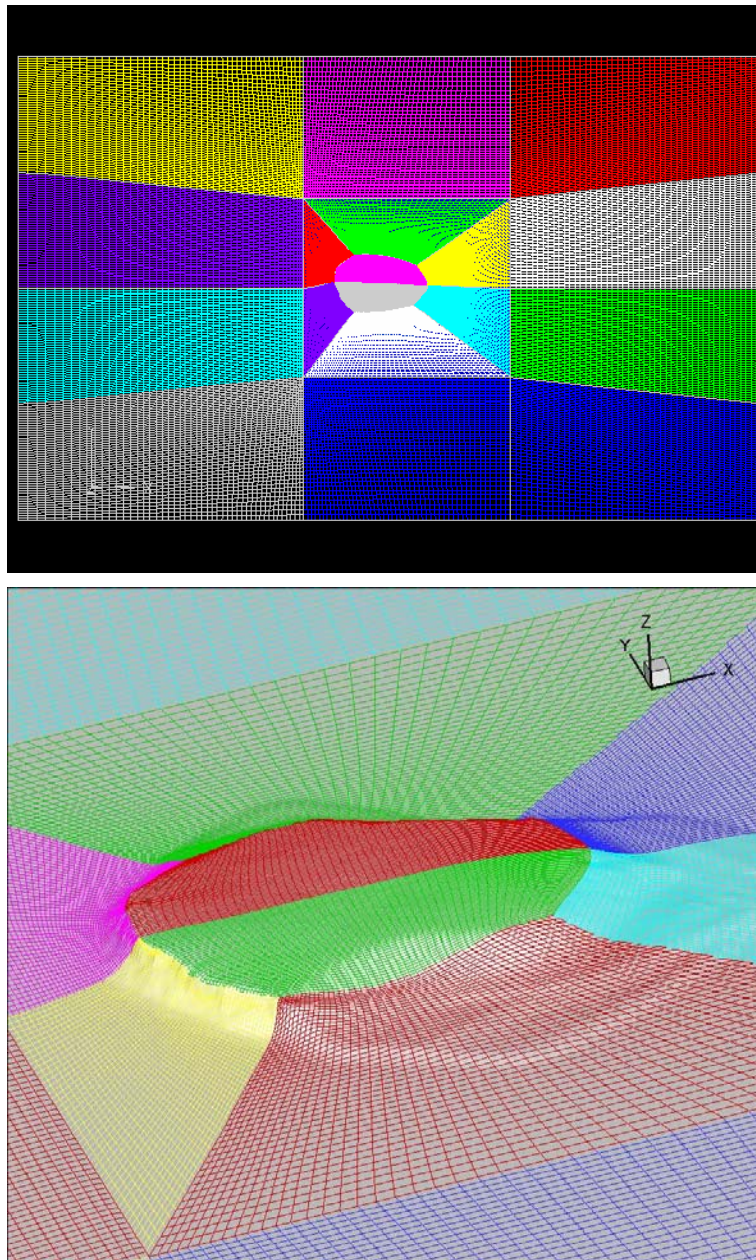


Figure 5. Top: The structured surface grid seen from above. The grid consists of 18 blocks. Bottom: Close-up of the surface grid around Bolund hill.

3.3 Volume grid

Finally, having generated the surface mesh, the in-house enhanced hyperbolic grid generator HypGrid3D is used to generate the final volume mesh. In the vertical direction 96 cells are used, giving a total of approximately 4 million cells and a cell height of 0.03 meter at the wall surface for the 400 m high domain, see Figure 6. The small cell height of the first near-wall grid cell is necessary in order to capture the large velocity gradients found over water. Since the domain height is about 30 times the hill height, unwanted boundary effects on near-hill wind is assumed negligible.

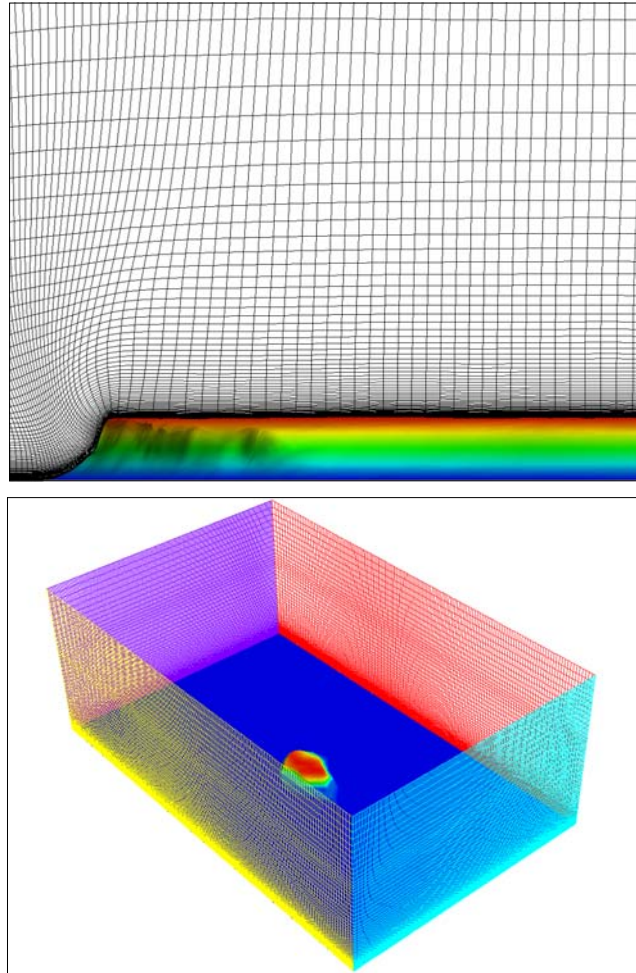


Figure 6. Top: The volume grid is generated by marching the surface grid in the vertical direction using HypGrid3D. Bottom: Overview of the computational domain

4 Boundary conditions

4.1 Inlet and top

Inflow conditions, using a standard logarithmic equilibrium profile, are assumed at the upstream face of the computational grid and at the top face of the computational domain. For the atmospheric boundary layer it is known that the logarithmic velocity profile is only “valid” at lower heights, i.e. in the surface layer ($\sim 80\text{m}$). However, since the height of the Bolund hill is low ($\sim 12\text{m}$) the logarithmic approximation is considered appropriate for these simulations. The logarithmic equilibrium profile for the velocity corresponds to the following condition,

$$U(z) = \frac{u_*}{\kappa} \ln\left(\frac{z}{z_0}\right) \quad (1)$$

where $\kappa = 0.4$ is the von Karman constant, u_* is the friction velocity and z_0 is the surface roughness height. In accordance with the logarithmic velocity profile the turbulent kinetic energy profile, $k(z)$, is specified as constant with a value given by,

$$k(z) = \frac{u_*^2}{\sqrt{C_\mu}}. \quad (2)$$

C_μ is a model constant that need to be specified. The equilibrium profile of the dissipation of turbulent kinetic energy is specified according to:

$$\varepsilon(z) = \frac{C_\mu^{\frac{3}{4}} k^{\frac{3}{2}}}{\kappa z}. \quad (3)$$

Since the inlet boundary is located at the sea we specify the surface roughness at the inlet as $z_0 = 0.0001\text{m}$, corresponding to calm sea. The friction velocity at the inlet is prescribed as $u_* = 0.347\text{ m/s}$, which results in a wind speed of $u = 10\text{m/s}$ in 10m height. Finally, $C_\mu = 0.03$ has been used (the standard value for atmospheric flow).

4.2 Outlet

At the outlet, fully developed flow is assumed. In the code this is implemented by using a zero gradient assumption in the mesh direction normal to the outlet plane.

4.3 Wall

The wall boundary condition is implemented using an assumption of the logarithmic velocity gradient in the vicinity of the wall, Eq. (1). However, unlike at the computational inlet, the friction velocity is not prescribed but is found as part of the solution. Details can be found in [3] and [4], which deals both with the velocities and the turbulent quantities.

5 Results

5.1 Flow visualisation

Figure 7 shows the simulated surface streamlines across Bolund for the 270° wind direction. As seen the flow stays attached over most of the hill. Flow separation is, however, found behind a small ridge to the south of the hill (red ellipse), in the hill wake and in a small region along the steep escarpment. Figure 8 shows iso-surfaces of high turbulence intensity for the two wind directions, 270° and 240°, respectively. For both directions a similar pattern is seen: High levels of turbulence are found just upstream of the escarpment, on the escarpment edge and in the hill wake. This characteristic turbulence pattern should be captured by the field experiment. An additional turbulence “tongue” is observed for the 270° direction, originating from the recirculation region behind the small ridge (red ellipse). Based on these plots, measuring mast positions have been proposed – shown as white dots on the figure.

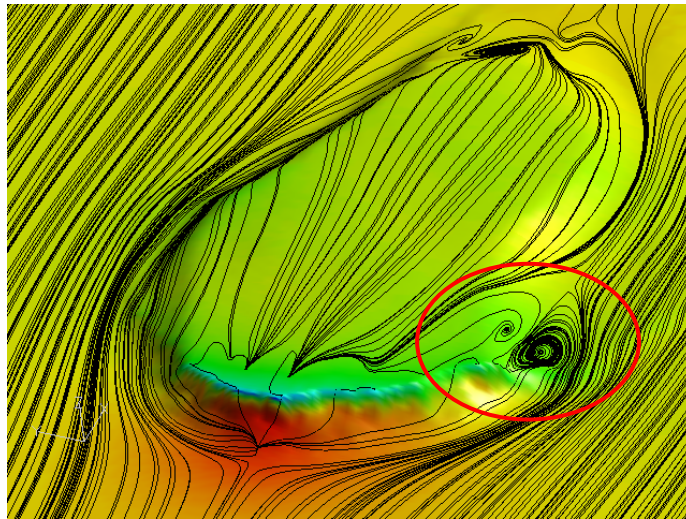


Figure 7. Surface streamlines. Wind direction 270°.

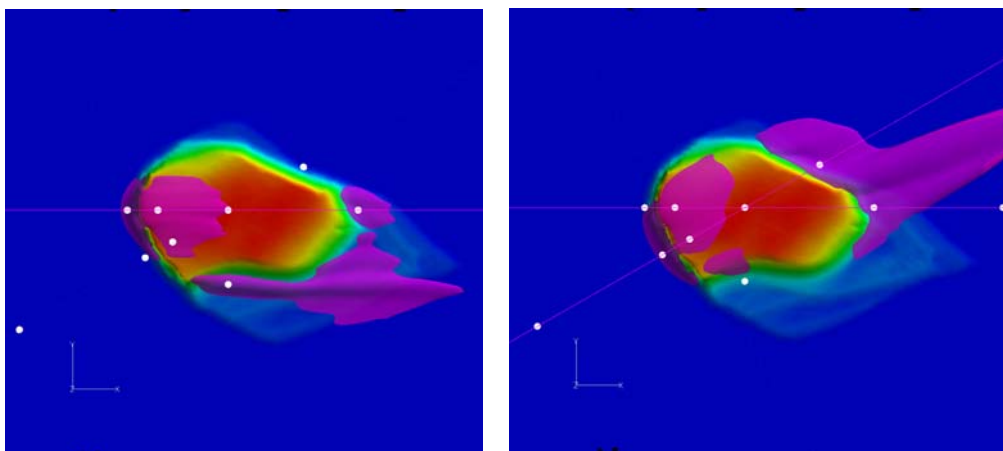


Figure 8. Iso-surfaces of high turbulence intensity. Left: dir 270°. Right: dir 240°.

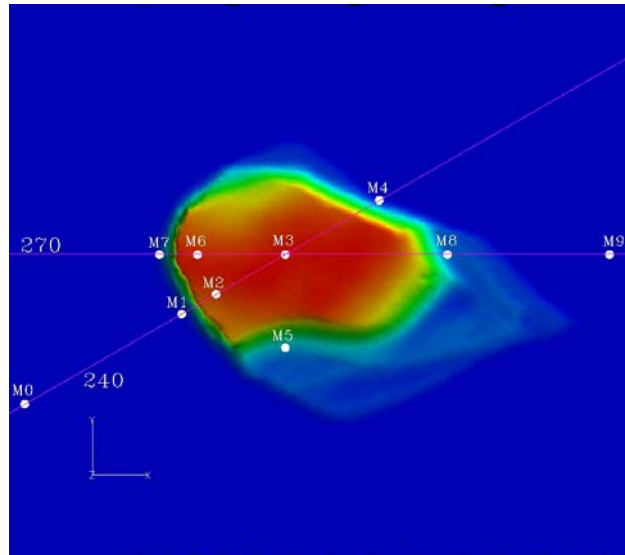


Figure 9. Close-up of mast positions

5.2 Location of measuring masts

Figure 9 shows a close-up of the mast layout with the two wind directions indicated. Mast M0 and M9 are needed in order to measure “undisturbed” wind conditions when wind comes from west and east. These masts need to be tall in order to have a proper estimate of free stream wind conditions. 16m masts are proposed. The other masts are located in lines along the predominant wind directions: M1, M2, M3, M4 for the 240° direction and M7, M6, M3, M8 for the 270° and 90° direction. Along these lines measurements will be made at the characteristic regions: 1. upstream of the escarpment, 2. on the escarpment edge 3. hill center and 4. in the hill wake. There are several reasons for having instrumentation on two lines parallel to the wind. The main reason is due to the relative limited time available for measurements. By having two lines a reasonable amount of usable experimental data should be achieved. Another reason is that different measurements are expected at the two lines. The escarpment geometry is straight and perpendicular to the wind for the 240° line, while it curves for the 270° line (see Figure 10). This may at first seem like a small difference but may have an effect on the flow at the escarpment edge. Finally, M5 is proposed in order to measure the wind in the recirculation zone.

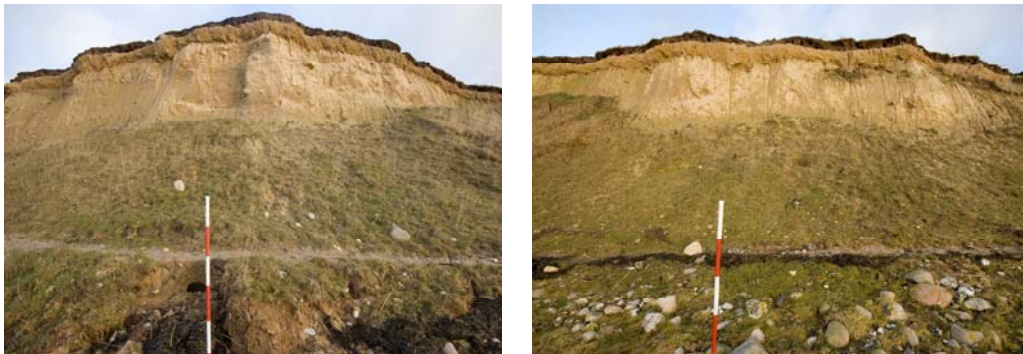


Figure 10. View from upstream of the escarpment. Left: 270 dir. Right: 240 dir.

5.3 Instrumentation

In order to determine mast heights and instrumentation, profiles of simulated wind speed, turbulence intensity and wind inclination has been extracted at the planned mast locations. These are shown on Figure 11 for the 240° and 270° directions. At the figure it is seen that the major deviations from the upstream values (at M0) of speed-up, wind inclination and turbulence intensity are found at heights of 5 meters and below. Large flow inclinations are observed at these heights, which makes measurements with cups unreliable. In order to measure the wind at these heights we therefore recommend that sonics should be placed in all masts at heights of 2 and 5 meter. The only exceptions are mast M0 and M9 where the sonics at 2 meter above ground have been cancelled. At these positions the turbulence intensity is expected to be constant with height and cup anemometers can be used to measure the mean wind since the wind inclinations are small.

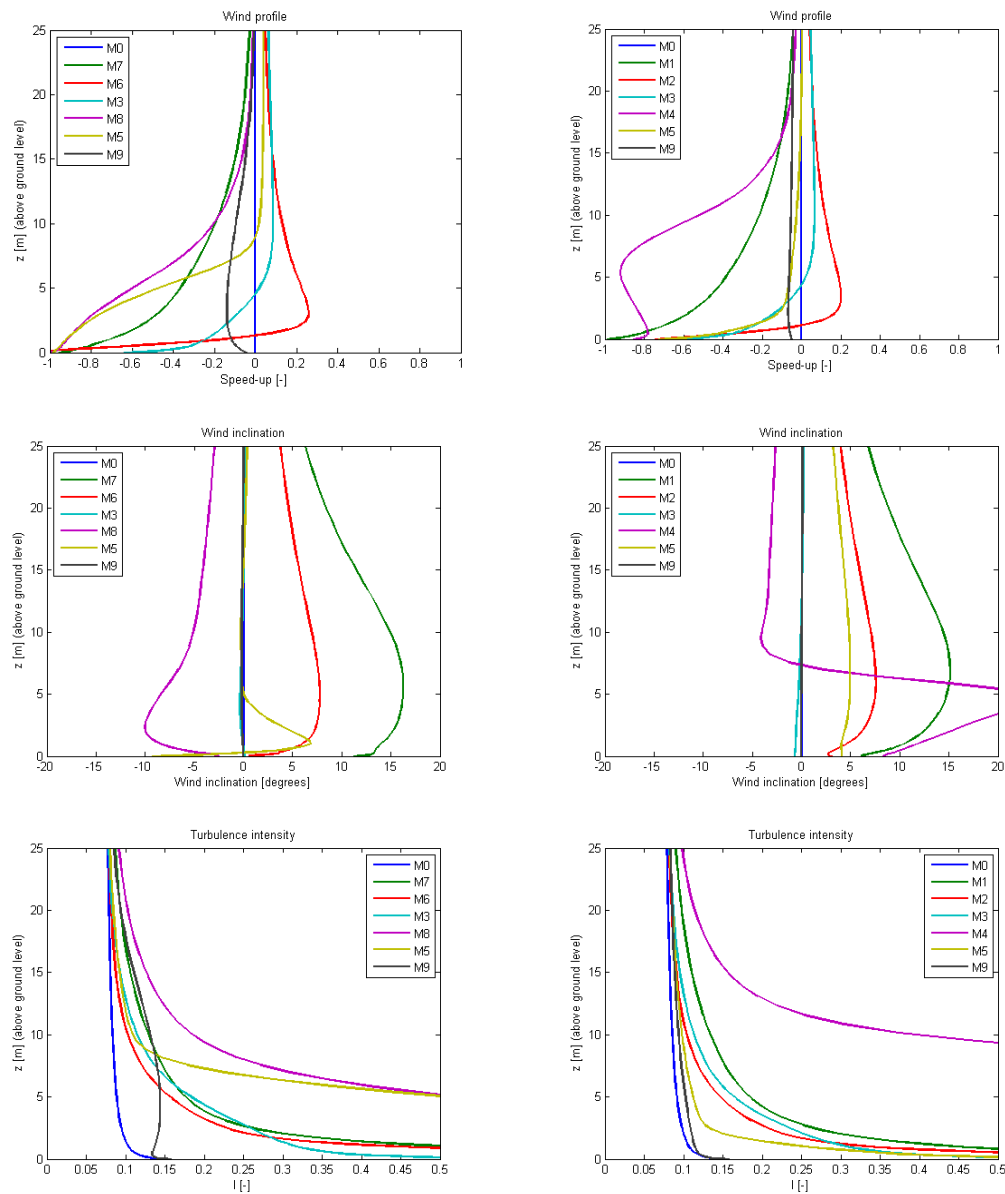


Figure 11. Profiles of speed-up, wind inclination and turb. intensity along line 270° (left) and 240° (right)

An additional sonic is placed at 1 meter height at M2 in order to investigate recirculation behind the escarpment edge.

Instruments are also proposed at 9 m height. Since the wind inclinations are small at this height most masts can be instrumented with cup anemometers. Mast M1 and M4 are, however, instrumented with sonics. The complete proposed distribution of measurement instruments is summarized in Table 1. In total the amount of measurement channels are: 21 Sonics and 12 cups located on two 16m masts, six 9m masts and two 5m mast.

Table 1. The proposed instrumentation: 0 corresponds to cup anemometers and X corresponds to sonic anemometers.

	1m	2m	5m	9m	16m	Position, N	Position, E
M0		0	0X	0	0	55°42'10.15''	12°05'44.88''
M1		X	X	X		55°42'12.10''	12°05'51.17''
M2	X	X	X	0		55°42'12.40''	12°05'52.23''
M3		X	X	0		55°42'13.05''	12°05'54.36''
M4		X	X	X		55°42'13.89''	12°05'57.25''
M5		X	X			55°42'11.46''	12°05'54.23''
M6		X	X	0		55°42'13.10''	12°05'51.72''
M7		X	X			55°42'13.10''	12°05'50.58''
M8		X	X	0		55°42'12.91''	12°05'59.50''
M9		0	0X	0	0	55°42'10.87''	12°06'12.82''

6 Discussion

CFD computations using EllipSys3D Navier-Stokes solver have been used to design a measurement campaign on the Bolund hill. Positions of measurement masts have been estimated based on areas of high turbulence intensity and suggestion to mast heights and their instrumentation was proposed based on profiles of speed-up, turbulence intensities and flow inclination.

Acknowledgement

The work is financed by the Danish Energy Agency under the project "EFP07 - Metoder til kortlægning af vindforhold i komplekst terræn". (ENS-33033-0062).

The CFD computations were made possible by the use of the Risø 240 nodes MARY PC-cluster and the computational resources of the Danish Centre for Scientific Computing at MEK/DTU in Lyngby.

References

- [1] Michelsen, J.A. "Basis3D - a Platform for Development of Multiblock PDE Solvers", Technical Report AFM 92-05, Technical University of Denmark, 1992.
- [2] Michelsen J.A., "Block structured Multigrid solution of 2D and 3D elliptic PDE's", Technical Report AFM 94-06, Technical University of Denmark, 1994.
- [3] Sørensen, N.N., "General Purpose Flow Solver Applied to Flow over Hills", Risø-R- 827-(EN), Risø National Laboratory, Roskilde, Denmark, June 1995.
- [4] Sørensen, N.N., Bechmann A., Johansen J., Myllerup L., Botha P, Vinther S and Nielsen B.S., "Identification of severe wind conditions using a Reynolds Averaged Navier-Stokes solver", Proceedings from "The Science of making Torque from Wind", Lyngby, Denmark, 28-31 August 2007
- [5] Rhie C.M. "A numerical study of the flow past an isolated airfoil with separation", Ph.D. thesis, Univ. of Illinois, Urbane-Champaign, 1981.
- [6] Patankar S.V. and Spalding D.B. "A Calculation Procedure for Heat, Mass and Momentum Transfer in Three-Dimensional Parabolic Flows." Int. J. Heat Mass Transfer, 15:1787,1972
- [7] Khosla P.K. and Rubin S.G., "A diagonally dominant second-order accurate implicit scheme", Computers Fluids, 2:207-209, 1974.
- [8] Launder B.E. and Spalding D.B.. The Numerical Compuation of Turbulent Flows. Comput. Meths. Appl. Mech. Eng., 3:269-289,1974.
- [9] Bechmann, A. Large-Eddy Simulation of Atmospheric Flow over Complex Terrain. Technical Report Risø-PhD-28(EN), Risø National lab., Roskilde, Denmark, 2006.

Risø's research is aimed at solving concrete problems in the society.

Research targets are set through continuous dialogue with business, the political system and researchers.

The effects of our research are sustainable energy supply and new technology for the health sector.

